


An Antibacterial, Conductive Nanocomposite Hydrogel Coupled with Electrical Stimulation for Accelerated Wound Healing

Dawei Ren¹, Yan Zhang¹, Bo Du¹, Lina Wang², Meiheng Gong¹, Wei Zhu¹ 

¹Department of Otorhinolaryngology, the First Hospital of Jilin University, Changchun, People's Republic of China; ²Department of Pediatric Respiration, the First Hospital of Jilin University, Changchun, People's Republic of China

Correspondence: Wei Zhu, Email zhuwei@jlu.edu.cn

Background: Electrical stimulation (ES) can effectively promote skin wound healing; however, single-electrode-based ES strategies are difficult to cover the entire wound area, and the effectiveness of ES is often limited by the inconsistent mechanical properties of the electrode and wound tissue. The above factors may lead to ES treatment is not ideal.

Methods: A multifunctional conductive hydrogel dressing containing methacrylated gelatin (GelMA), Ti_3C_2 and collagen binding antimicrobial peptides (V-Os) was developed to improve wound management. Ti_3C_2 was selected as the electrode component due to its excellent electrical conductivity, the modified antimicrobial peptide V-Os could replace traditional antibiotics to suppress bacterial infections, and GelMA hydrogel was used due to its clinical applicability in wound healing.

Results: The results showed that this new hydrogel dressing (GelMA@ Ti_3C_2 /V-Os) not only has excellent electrical conductivity and biocompatibility but also has a durable and efficient bactericidal effect. The modified antimicrobial peptides V-Os used were able to bind more closely to GelMA hydrogel to exert long-lasting antibacterial effects. The results of cell experiment showed that the GelMA@ Ti_3C_2 /V-Os hydrogel dressing could enhance the effect of current stimulation and significantly improve the migration, proliferation and tissue repair related genes expression of fibroblasts. In vitro experiments results showed that under ES, GelMA@ Ti_3C_2 /V-Os hydrogel dressing could promote re-epithelialization, enhance angiogenesis, mediate immune response and prevent wound infection.

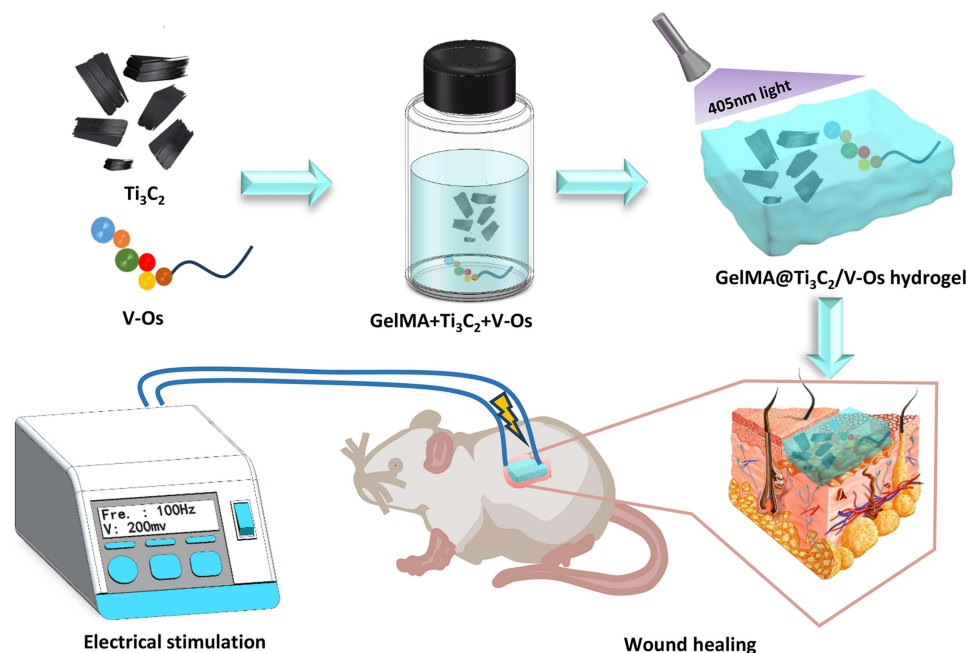
Conclusion: This multifunctional nanocomposite hydrogel could provide new strategies for promoting infectious wound healing.

Keywords: MXene, GelMA, electrical stimulation, antimicrobial peptides, wound healing

Introduction

Skin is the largest organ of the human body and the first line of defense against infection and infringement of the external environment.¹ Once skin damage occurs, the integrity and homeostasis of the skin tissue will be compromised. Most skin wounds heal themselves through four stages: hemostasis, inflammation, cell proliferation, maturation, and remodeling.^{2,3} However, when skin wounds are improperly treated or in poor health, such as aging, diabetes, or vascular disease, even a small wound can develop into a chronic wound and may not heal for years due to excessive inflammation, persistent infections, and other injuries.⁴ The healing process of chronic wounds is usually longer, often staying in the inflammatory period, which is easy to cause the deterioration of the original wound. There are many treatments for skin wounds, and the most common treatment strategy is to cover and protect the skin wound area with wound dressings. The physical and chemical properties of wound dressings can also regulate the wound microenvironment, thus promoting skin wound healing.⁵ Among various wound dressings, hydrogel dressings have a structure similar to extracellular matrix, have good biocompatibility, can absorb wound exudate, and provide a moist environment around the wound, so they are widely used in the treatment of skin wounds.^{6,7} At the same time, the hydrogel dressing can also be used as a carrier of bioactive factors or antibacterial drugs to improve the skin healing rate.⁸ Adjuvant treatments such as electrical stimulation (ES)

Graphical Abstract



are also often used to treat skin wounds. Some studies have found that ES can accelerate wound healing by enhancing the proliferation and migration of fibroblasts, which in turn encourages keratinocytes to secrete more extracellular matrix.^{9,10} At the same time, ES can activate cellular ion channels and downstream transduction signals to guide the migration and proliferation of skin cells, especially epithelial cells and fibroblasts.¹¹ Therefore, ES is also an effective treatment for accelerating skin regeneration.

Based on the respective advantages of ES and hydrogel dressings, the study of their combined application in the treatment of skin injury has become more and more common. However, most hydrogel materials have poor electrical conductivity and cannot effectively guide the conduction of ES in the damaged tissue. Furthermore, hydrogel dressings alone lack the necessary antibacterial and biological activity to maximize the rate of skin wound healing. These factors limit the application of ES combined with hydrogels in skin wound treatment. In order to solve these problems, it is necessary to add some bioactive ingredients to the hydrogel dressing. Currently, various conductive materials, such as conductive polymers, carbon-based materials, and metal-based materials, have been introduced into hydrogels to enhance the conductivity of the material.^{12–14} Among various conductive materials, MXene (Ti₃C₂) has attracted much attention in recent years. Ti₃C₂ is a novel two-dimensional layered material with a layered structure similar to graphene.^{15,16} Ti₃C₂ has good electrical conductivity, which can greatly improve the electrical activity of the material to meet the requirements of current conduction on the wound surface. Ti₃C₂ also has good antibacterial properties and can kill both gram-positive and gram-negative bacteria.^{17,18} In addition, Ti₃C₂ can significantly reduce the production of ROS, so adding Ti₃C₂ to the hydrogel can give it some antioxidant capacity, which can reduce the degree of inflammation at the site of skin wound.¹⁹ Therefore, the introduction of Ti₃C₂ into hydrogel dressings is expected to improve the material's electrical conductivity, antibacterial activity and biological activity and further accelerate wound healing. In the treatment of skin wounds, another major factor affecting wound healing is infection. Bacterial infection can cause the increase of exudate at the wound site and inhibit the formation of granulation tissue.^{20,21} Antimicrobial peptides (AMPs) are a natural antimicrobial immune system.²² AMPs exert antibacterial activity through non-targeted membrane cleavage mechanism and does not lead to the generation of drug-resistant bacteria. AMPs have broad spectrum antibacterial ability, good biocompatibility and low drug resistance and are a potential substitute for antibiotics. However, AMPs as a polypeptide has the same

defects as growth factors, such as a short half-life and poor stability when combined with other materials. In recent years, a method to improve the binding ability of polypeptide substances by introducing specific protein sequences into polypeptides has been widely used.^{23,24} This method avoids the sudden release and inactivation of the drug. Therefore, we speculate that this method can improve the binding affinity of recombinant AMPs with hydrogel dressings, and further expand the application range of hydrogel dressings.

Based on the above research background, we developed a novel conductive, injectable and antibacterial multi-functional methacrylated gelatin (GelMA) hydrogel dressing (GelMA@Ti₃C₂/V-Os) and used it in combination with ES. The introduction of MXene into hydrogels will improve the conductivity and biocompatibility of hydrogels. At the same time, we introduced collagen molecules into antimicrobial peptide Os, prepared recombinant antimicrobial peptide (V-Os), and loaded V-Os into GelMA hydrogel, which will improve the antibacterial properties of hydrogel dressing. The surface morphology, electrical conductivity and biocompatibility of GelMA@Ti₃C₂/V-Os hydrogel dressing were studied. The antibacterial properties of the hydrogel dressing were tested with *E. coli* and *S. aureus*. The effect of hydrogel dressing combined with ES on infected skin wound was evaluated by the model of full-layer skin defect in rats. We believe that this electroactive hydrogel dressing with good biocompatibility and multiple functions combined with ES therapy can enhance the therapeutic effect of each other and accelerate the healing of skin tissue to the greatest extent. This combined treatment method has a broad application prospect in the treatment of skin injury.

Materials and Methods

Materials

Ti₃C₂ was purchased from Jilin 11 Technology Co., Ltd (Changchun, China). GelMA was purchased from SunP Biotech Co., Ltd (Beijing, China). The peptide Os (KGIRGYKGGYCKGAFKQTCKCY), FITC-labelled Os (FITC-Os), WREPSFCALS-Os (V-Os) and FITC-labelled V-OS (FITC-V-Os) were synthesized by BGI Co., Ltd. (Wuxi, China). Reagents associated with cell experiments were purchased from Solarbio Technology Co., LTD (Beijing, China). NIH3T3 cells purchased from the Cell Culture Centre of Institute of Basic Medical Sciences Chinese Academy of Medical Sciences (Shanghai, China). *Escherichia coli* (*E. coli*) and *Staphylococcus aureus* (*S. aureus*) were purchased from Solarbio Technology Co., LTD (Beijing, China).

Preparation of GelMA@Ti₃C₂/V-Os Hydrogels Dressing

E. coli and *S. aureus* were used as strains to evaluate the antibacterial ability of different concentrations V-Os. Different weights of V-Os were added to the bacterial solution, and the final solution concentrations of V-Os reached 31.25, 62.5, 125, 250 and 500 µg/mL, respectively. After 24 hours of culture, the absorbance value of the bacterial solution at 600 nm was detected by multifunctional microplate reader (M200, Tecan, Switzerland), and the antibacterial rate of the sample was calculated. GelMA is dissolved in dd H₂O (10%, W/V) containing 2% Ti₃C₂ and the mixed solution is thoroughly stirred at 60°C. After GelMA is completely dissolved, wait until the temperature decrease to 37°C, 250 µg of V-Os was added to 1mL mixture containing GelMA and Ti₃C₂. The solution was cross-linked by 405 nm blue light irradiation for 10s to form GelMA@Ti₃C₂/V-Os hydrogels. GelMA, GelMA@ Ti₃C₂ and GelMA@V-Os hydrogels were prepared in the same way.

Hydrogels Dressing Characterization

The sol-gel transition state of the hydrogel was observed by the vial tilting method. The surface topography of the hydrogel was observed by scanning electron microscopy (SEM, Zeiss EVO 18, Germany). The internal structure of hydrogel was observed by micro-CT (Scansky1172, Bruker). The conductivity of hydrogel was determined by cyclic voltammetry and electrochemical workstation. The hydrogel is cut with a knife, and the broken surface is reconnected to visually observe the conductivity of the hydrogel. Fourier transform infrared spectroscopy (FTIR, Bruker, Germany) is used to detect the chemical composition of hydrogels. The Ti₃C₂ was determined by X-ray photoelectron spectroscopy (XPS, D8 ADVANCE, Bruker, Germany) and Transmission electron microscope (TEM, JEOL 2100, Japan). FITC-Os and FITC-V-Os were mixed into GelMA hydrogel to evaluate the binding ability of AMPs with hydrogel. AMPs in the

hydrogel were photographed using a fluorescent in vivo imager (IVIS Lumina LT IVIS, PE, US). The surface hydrophilicity of different hydrogel materials was measured by contact angle analyzer (DSA25, Kruss, Germany). The mechanical properties of hydrogel materials were measured by universal mechanical tester (AGS-X100 N; SHIMADZU, Japan). Different groups of lyophilized hydrogels were immersed in PBS for 10 hours, and then the swelling hydrogels were weighed. Swelling ratio was calculated by formula (1):

$$\text{Swelling ratio (\%)} = [(W_s - W_D) / W_s] \times 100\% \quad (1)$$

Where W_s is the weight of the swelling hydrogel and W_D is the weight of the lyophilized hydrogel.

Determination of Antibacterial Activity

Using *Escherichia coli* (*E. coli*) and *Staphylococcus aureus* (*S. aureus*) as strains, the antibacterial properties of different hydrogel dressings were evaluated. In brief, different hydrogels were sterilized with ultraviolet light. The concentration of bacteria was adjusted to 5×10^6 CFU/mL and cultured in a constant temperature incubator at 37°C for 2 h, and then the bacteria solution was co-cultured with the sterilized hydrogel. After 7 h, the bacterial solution was absorbed and diluted. The 30μL diluted bacterial solution was then evenly applied to the LB culture plate and incubated at 37°C overnight. Subsequently, the colonies on LB culture plate were observed and photographed, and the antibacterial rate of different hydrogels was evaluated according to the number of colonies. To further evaluate the antibacterial activity of different hydrogels in vivo, we made a 1cm wound on the skin of rats and added 50μL (10^6 CFU bacteria/mL) of *E. coli* solution to the wound. Different groups of 0.2g hydrogels were implanted into the bacterial-containing wound, and the wound was then sutured. After 3 days, the experimental animals were killed, and the tissues around the wound were excised and sliced. Finally, the skin tissue was stained with gram staining method, and the skin tissue sections were observed.

Cell Proliferation, Migration and Adhesion Assays

In vitro cell ES device was purchased from Ubbiotech Co., LTD. (Changchun, China). A pair of platinum electrodes were installed on the lid of the 24-well cell culture plate, and the electrode distance was 1cm. The ES signal source was generated by a function signal generator (RIGOL DG1022, China). The frequency, voltage and waveform of ES signal were monitored by oscilloscope (RIGOL DS1102, China). Cell Counting Kit-8 (CCK-8) assay and Calcein AM staining were used to detect the effects of different hydrogels and voltage on the proliferation and adhesion of NIH3T3 cells. In brief, NIH3T3 cells (4×10^4 cells/wells) were seeded in a 24-well plate containing different hydrogel at 37°C and 5% CO₂ for 24 h. Electrical signals of 100Hz, square wave and voltage (0, 100, 200 and 400 mv) were applied to the cells through the platinum electrode and stimulated for 1h every day for 3 days. After 3 days of cell culture, CCK-8 was used to detect cell proliferation. First, the medium was removed; then, 500μL of CCK-8 working solution prepared using cell culture medium was added. Next, the cells were incubated at 37°C for 2 h. Absorbance was measured at 450 nm using a multi-function plate reader (M200, Tecan, Switzerland). To evaluate cell adhesion, NIH3T3 cells were cultured on different hydrogel material under ES for 3 days, and then the medium was discarded, and the samples were cleaned with PBS. Finally, the cells were stained with 2μM Calcein AM solution for 10 min. Finally, the cells were cleaned again with PBS, and cells on different sample surfaces were observed under fluorescence microscope (TE-2000U, Nikon, Japan).

Real-Time Quantitative PCR Analysis

To further quantitatively analyze the wound repair related genes expression of cells under different conditions, RNA was extracted using TRIzol reagent (Invitrogen, USA) according to the manufacturer's protocol. Total RNA concentration and purity were determined by a NanoDrop spectrophotometer (M200, Tecan, Switzerland). RNA samples were reverse-transcribed into cDNA using PrimeScript kit (Takara, China) for qRT-PCR. The qRT-PCR program started with denaturation at 95 °C for 10 min, followed by 40 cycles at 95 °C for 30s, 58 °C for 1 min, and 72 °C for 1 min. Beacon 5.0 primer design software was used to design gene-specific primers including glyceraldehyde-3-phosphate dehydrogenase (GAPDH), type 1 collagen (COL-I), and vascular endothelial growth factor (VEGF) (Table 1). The

Table I List of Genes and Primer Nucleotide Sequences

Gene		Primer Sequences
VEGF	Forward	5-CCTTCAGCTCGCTCCTCC ₋₃
	Reverse	5-GAAGATGAGGAAGGGTAAGCC ₋₃
COL-I	Forward	5- CTGAAATGTCCACCAGCC ₋₃
	Reverse	5- GTCCGATGTTTCCAGTCTGC ₋₃
GAPDH	Forward	5-CCTTCCGTGTTCTACCCC ₋₃
	Reverse	5- ACCAGGAAATGAGCTTGACA ₋₃

expression values of each gene were normalized with those of the steward gene GAPDH. The results were reported as relative gene expression. All experiments were done three times to obtain average data.

Establishment and Treatment of a Full-Thickness Wound

The experimental animals were selected as healthy 8-week-old female SD rats, and all the experimental animals were purchased from Liaoning Changsheng Biotechnology Co., Ltd. All procedures and plans for animal experiments follow the guidelines on the care and experimental animals of China and are approved by the Animal Protection and Use Committee of Jilin University. The experimental animals were divided into 5 groups: GelMA, GelMA@V-Os, GelMA@Ti₃C₂, GelMA@Ti₃C₂/V-Os and GelMA@Ti₃C₂/V-Os+ES. Before operation, rats were anesthetized by inhalation using isoflurane and anesthesia machine (RWD, China). After removing the skin hair on the back, a full-layer wound with a diameter of 10 mm were created on each rat and divided into different treatment groups. After the full-layer skin wound model of rats was established, different hydrogels (GelMA, GelMA@Ti₃C₂, GelMA@V-Os, GelMA@Ti₃C₂/V-Os) were implanted on the skin wound surface and covered with sterile gauze. In the ES group, electrodes were inserted into both ends of the skin wound and fixed with bandages. The rats were treated with ES (100 Hz, 200 mv and square wave) for 1 h every day under gas anesthesia, ensuring that the electrodes were always at both ends of the skin wound during the treatment. After 3, 6, 9 and 11 days of treatment, the wound was photographed, and the area of the wound was calculated using Image J software. Finally, the wound healing rate (%) was calculated according to the formula (2).

$$\text{Wound healing rate \%} = [(A_0 - A_t)/A_0] \times 100\% \quad (2)$$

Where A_0 is the initial area of the wound at day 0, and A_t is the wound area at the measurement time.

Histopathological Assay

After 11 days, the rats were killed, and the skin samples of the wound site were taken and carefully trimmed with the cutter. Skin samples were fixed with paraformaldehyde and were then placed in paraffin wax and cut into tissue slices. Subsequently, skin samples were stained by Masson and H&E staining. To evaluate wound inflammation and angiogenesis, immunofluorescence staining was performed on sections with anti-CD31 antibody (Abcam, UK) and TNF- α antibody (Abcam, UK). Furthermore, in order to observe the deposition of collagen on the wound, the tissue samples were stained with Sirius red and observed under a polarizing microscope. The proportion of type I and type III collagen was quantitatively analyzed. Finally, in order to analyze the biological toxicity of different hydrogel materials, different hydrogel materials were implanted into the muscle tissue of rats, and the rats were killed one month later. The important internal organs of the rats (heart, liver, spleen, lung and kidney) were removed, sliced and stained by H&E, and finally observed under a microscope and compared with the internal organs of normal rats.

Statistical Analysis

All quantitative data and plot graphs were analyzed and generated by Origin 8.0 software (Origin Lab Corporation, USA) and expressed as mean \pm standard deviation. One-way analysis of variance was used for more than two variables, and the t -test was used for two variables. $*P < 0.05$ was considered statistically significant.

Results and Discussion

Characterization of the GelMA@Ti₃C₂/V-Os Hydrogels Dressing

As shown in Figure 1A, GelMA@Ti₃C₂/V-Os solution is a viscous liquid before crosslinking. After illumination by 405 nm blue light, the solution was cross-linked and solidified. The microstructure of GelMA@Ti₃C₂/V-Os hydrogel was observed by SEM and micro-CT. As shown in Figure 1B and C, GelMA@Ti₃C₂/V-Os hydrogel has an obvious porous structure inside, which facilitates the transport of nutrients and the removal of metabolic wastes. The porosity of hydrogels in each group was about 89%. The surface morphology of GelMA and GelMA@V-Os hydrogels is not significantly different. The structure of Ti₃C₂-containing hydrogels is significantly more compact than that of GelMA and GelMA@V-Os hydrogels with loose structure, and the synergistic effect between the compact cross-structure, complex physical entanglements and strong chemical bonds is the key to improve the strength of hydrogels. Some rough particles can be found on the surface of the hydrogel containing Ti₃C₂, which may be formed by Ti₃C₂ agglomeration. This rough surface structure can provide more adhesion sites for cells and can improve the adhesion behavior of cells to a certain extent.

Then, FTIR and XPS were used to detect the chemical composition of different hydrogel materials. GelMA is a functionalized form of gelatin protein. Peptides and proteins are typically characterized by repeating units called amides 1, 2, etc. As shown in Figure 2A, FTIR results of GelMA sample showed peaks at 3267, 3076, 2936, 1633, 1533, 1446, 1403, 1335, 1236, 1080, and 1024 cm⁻¹. After the addition of the V-Os to the GelMA hydrogel, there was no significant change in the FTIR characteristic peaks, which may be due to the fact that V-Os is also a protein substance and its characteristic peaks overlap with GelMA. Figure 2B shows the TEM image of the Ti₃C₂ nanomaterial, indicating that the synthesized Ti₃C₂ nanomaterial presents a thin sheet with sharp edges. XPS (Figure 2C) results show that the main components of Ti₃C₂ are Ti and C. As shown in Figure 2D, different intensity visible fluorescence signals (Avg Signal) can be seen in the image, and fluorescence intensity represents the peptide content. The results showed that the

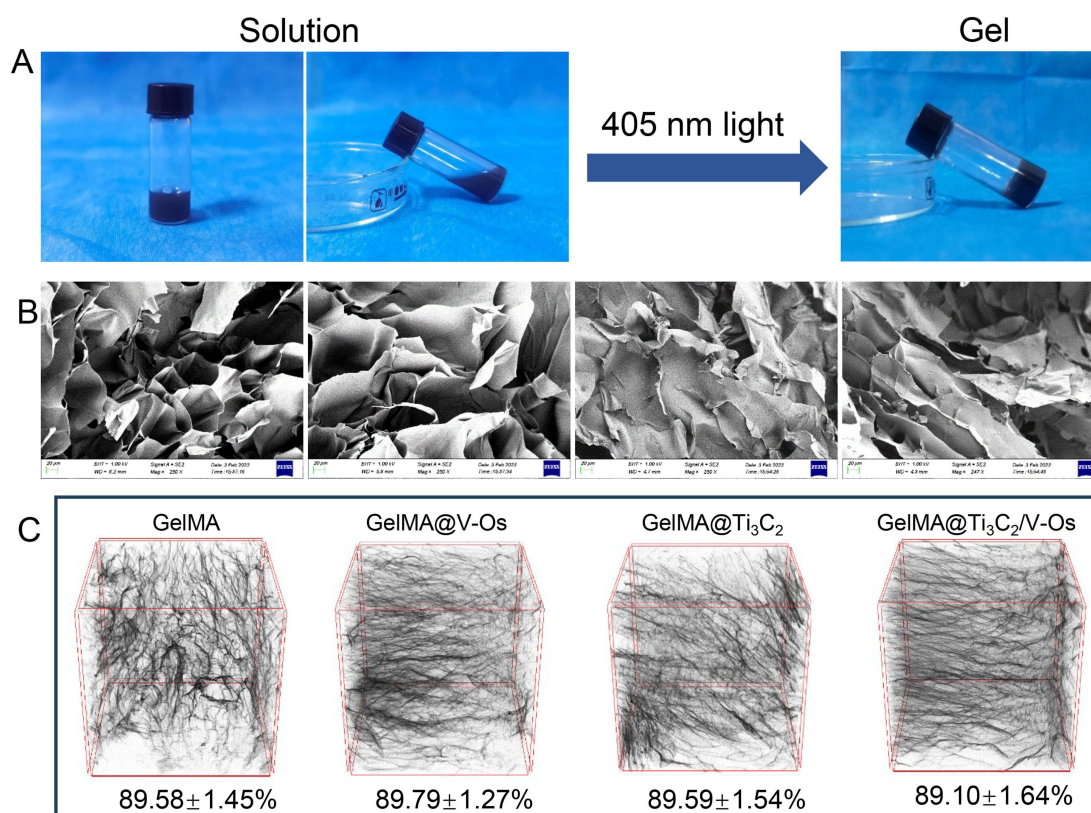


Figure 1 (A) Images of the GelMA@Ti₃C₂/V-Os solutions and the GelMA@Ti₃C₂/V-Os hydrogels. (B) SEM and (C) micro-CT images and porosity of different group hydrogels, the scale length is 20μm.

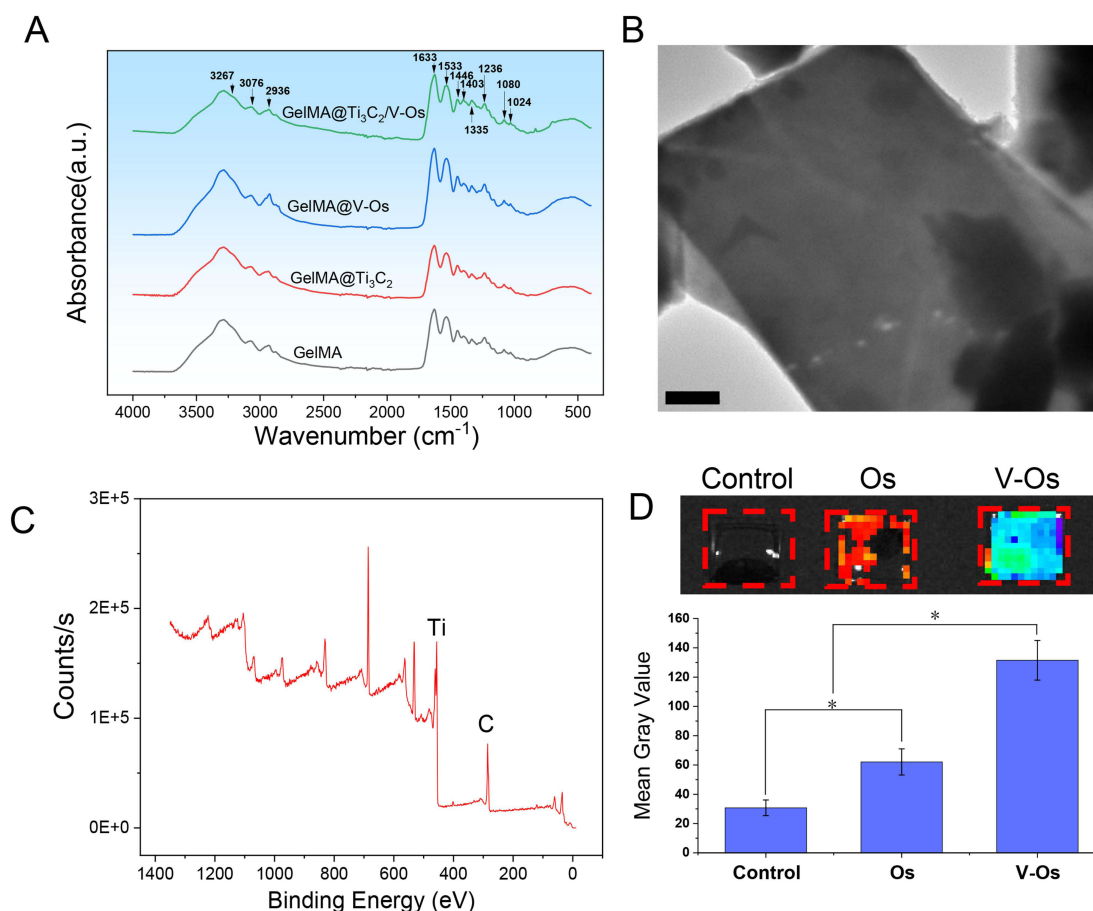


Figure 2 (A) FTIR spectrum of different hydrogels, (B) TEM image of Ti₃C₂ sample, (C) XPS survey and (D) the binding ability of V-Os and Os with GelMA hydrogels (**P* < 0.05, *n*=3).

fluorescence intensity was strongest in V-Os group, followed by Os group, and there was basically no fluorescence signal in negative control group. From the quantitative value, it is found that the Avg Signal of V-Os group is 2.12 times than that of Os group. Therefore, V-Os can more tightly bind to GelMA hydrogel, and this special binding ability can prevent the sudden release and inactivation of antimicrobial peptides. As an inherent substance of the immune system, AMPs are widely used in the antibacterial treatment of skin wounds because of its good biocompatibility and antibacterial properties. Os is an antimicrobial peptide with good broad-spectrum antibacterial activity but does not affect the growth of most eukaryotic cells.^{25,26} Os can be used as an effective bioactive factor to modify the surface of polymer materials, and its antibacterial activity can inhibit the growth of bacteria at the wound site. In this study, Os was used to improve the antibacterial ability of GelMA hydrogel. At the same time, in order to improve the binding stability of antimicrobial peptide Os and GelMA hydrogel, a kind of collagen-binding domain was introduced into Os to prepare GelMA binding V-Os.

The hydrophilicity of dressing materials has a significant effect on cell adhesion and proliferation. In general, a suitable hydrophilic surface can create a better cell microenvironment for cell growth.²⁷ By measuring the water contact angle on different hydrogel, the wettability of different hydrogel can be determined. As shown in Figure 3A and B, the contact angle of GelMA hydrogel was $67.5 \pm 3.02^\circ$. After adding V-Os and Ti₃C₂ to the hydrogel, the hydrophilicity of hydrogel did not change significantly. Some studies have found that when the contact angle of the material is about 65° , its surface is most conducive to the adhesion of cells, while both high and low contact angles are not conducive to the adhesion of cells.²⁸ The contact angle of GelMA@Ti₃C₂ and GelMA@Ti₃C₂/V-Os group were $64.77 \pm 3.06^\circ$ and $64.37 \pm 5.88^\circ$, so we speculated that cells could better adhere and grow on the surface of GelMA@Ti₃C₂/V-Os hydrogel. The mechanical properties of dressings are also important factors in wound healing. In the process of wound healing, the dressing materials should have

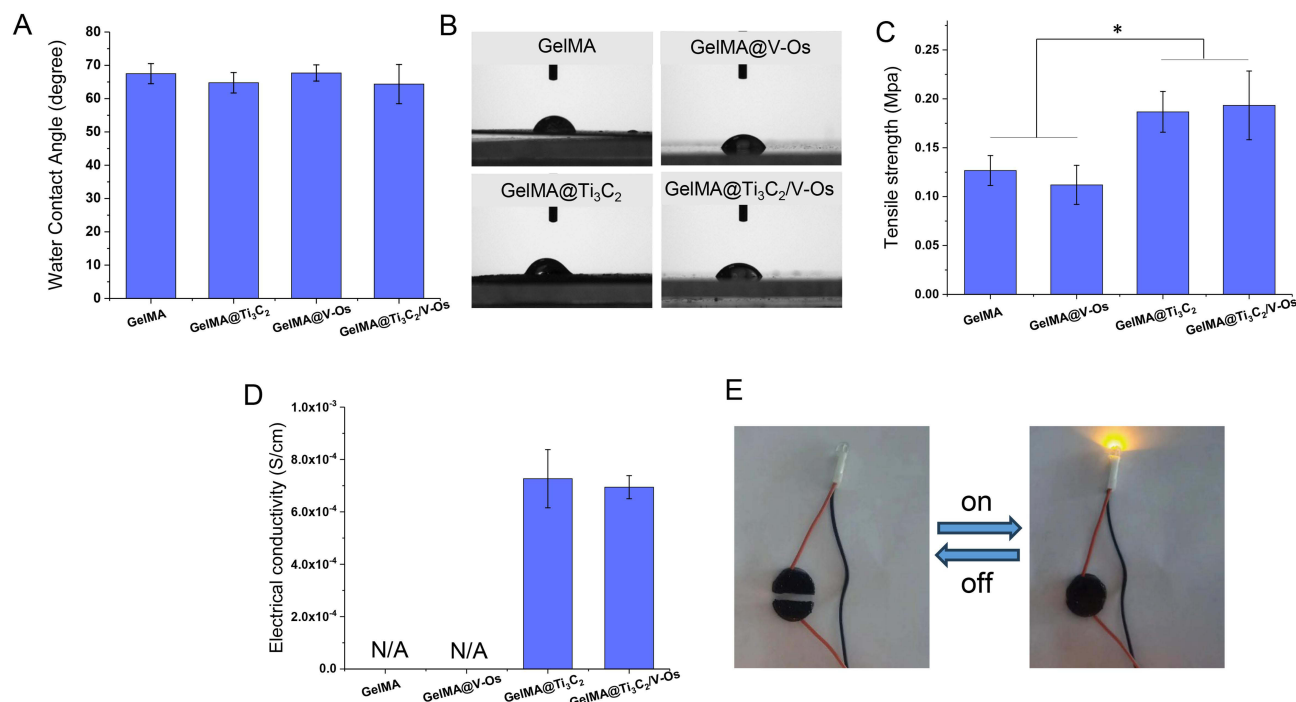


Figure 3 (A and B) Water contact angle, (C) mechanical tensile results and (D) electrical conductivity results of different hydrogels. (E) The display of the conductivity ability of GelMA@Ti₃C₂/V-Os hydrogels. (**P* < 0.05, *n* = 3).

appropriate mechanical strength to adapt to the deformation caused by wound contraction.²⁹ In order to study the effects of V-Os and Ti₃C₂ on the mechanical properties of GelMA hydrogels, we tested the tensile strength of different hydrogels. As shown in Figure 3C, the tensile strength of GelMA, GelMA@V-Os, GelMA@Ti₃C₂ and GelMA@Ti₃C₂/V-Os hydrogels are 0.127 ± 0.015, 0.112 ± 0.020, 0.187 ± 0.021, and 0.193 ± 0.035 MPa, respectively. The addition of Ti₃C₂ can significantly enhance the mechanical properties of hydrogel materials. Previous studies have found that there is a strong interface interaction between MXene and many polymer materials, and the stress of composite materials can be effectively transferred through MXene.³⁰ Many studies have found that electroactive materials are more conducive to the exchange of information between cells.^{31,32} Therefore, the electrical conductivity of different hydrogel materials is detected. As shown in Figure 3D, the conductivity of GelMA and GelMA@V-Os hydrogel is close to zero, and the conductivity of hydrogels containing Ti₃C₂ is 7.27 × 10⁻⁴ Sm⁻¹ and 6.94 × 10⁻⁴ Sm⁻¹, respectively. At the same time, we cut the round sheet GelMA@Ti₃C₂/V-Os hydrogel into two segments and then put the two segments back together (Figure 3E). The conductivity of GelMA@Ti₃C₂/V-Os hydrogel was also recovered very well, because the brightness of the yellow light plate hardly changed before and after the hydrogel healed. This result further proves that GelMA@Ti₃C₂/V-Os hydrogels have good electrical conductivity. Due to the low microcurrent intensity of the human body, the prepared scaffold material can fully meet the conduction of electrical signals between cells in the body. As shown in Figure S1, the swelling ratios of hydrogels were evaluated. The swelling ratios of GelMA, GelMA@V-Os, GelMA@Ti₃C₂ and GelMA@Ti₃C₂/V-Os hydrogels were 317.5 ± 22.1%, 306.1 ± 15.6%, 342.8 ± 17.3, and 351.2 ± 25.1%, respectively. There was no significant difference in swelling ratios among all groups, but the swelling rates of the hydrogels containing Ti₃C₂ were slightly higher than GelMA, GelMA@V-Os groups.

Antimicrobial Properties of GelMA@Ti₃C₂/V-Os Hydrogels Dressing

To determine the optimal loading of V-Os in GelMA hydrogels, we prepared hydrogels containing 31.25, 62.5, 125, 250 and 500 µg/mL V-Os, respectively. Then, bacteria were co-cultured different hydrogels. As shown in Figure S2, after loading V-Os, all hydrogels could inhibit the growth of pathogenic bacteria to a certain extent, and when the concentration of V-Os was 62.5 µg/mL, the antibacterial rate of hydrogels was 50%. With the continuous increase of V-Os

concentration, the antibacterial rate of hydrogel was further enhanced, but there was no significant difference between 250 and 500 $\mu\text{g/mL}$ groups. Considering that excessive high concentration of antibacterial peptides may have a negative effect on cell activity, we selected a minimum concentration of 250 $\mu\text{g/mL}$ as the best parameter for subsequent hydrogel preparation.

As shown in Figure 4A-C, a large number of colonies were formed on the culture plates of GelMA group, and the bacterial survival rate reached 100%, indicating that the GelMA hydrogel itself had no obvious antibacterial activity. In the GelMA@Ti₃C₂ group, the number of colonies was significantly reduced, and the bacterial activity decreased to less than 60%. These results indicated that Ti₃C₂ had a certain bactericidal effect, which might involve the disruption of the peptidoglycan network on the bacterial cell wall.³³ Many studies have found that Ti₃C₂ has strong antibacterial properties

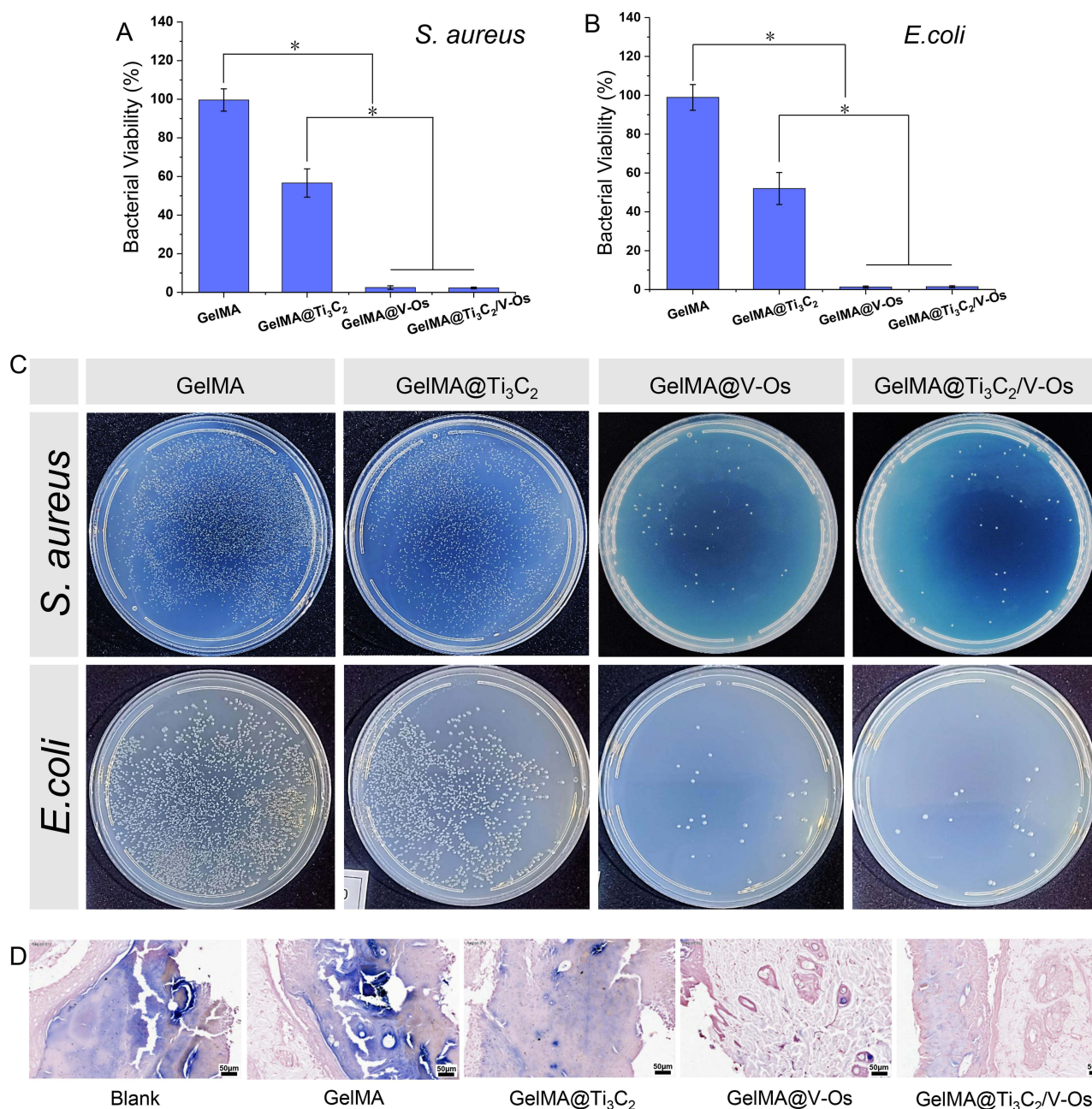


Figure 4 (A and B) Bacterial viability and (C) the colony growth of *E. coli* and *S. aureus* in different hydrogel. (D) H&E staining of the skin tissue embedded with different hydrogel after the wound site was infected with bacteria, the scale length is 20 μm . (* $P < 0.05$, $n=3$).

and can inhibit the growth of bacteria. The hydrophilicity and anion surface of Ti_3C_2 enhance its interaction with bacterial cell membranes. Hydrogen bonds between lipopolysaccharide molecules in cell membranes and Ti_3C_2 functional groups can inhibit bacterial growth by preventing nutrient intake and resulting in cell inactivation.³⁴ Furthermore, the oxidation of Ti_3C_2 in air leads to the formation of sharp TiO_2 nanocrystals, further enhancing its antimicrobial properties.¹⁸ Another theory proposes that MXene forms free radicals when it contact with bacteria, causing oxidative stress on the surface of the bacteria and thus killing them.³⁵ In the GelMA@V-Os and GelMA@ Ti_3C_2 /V-Os group, only a few colonies were found, and the bacterial activity was close to 0, which indicated that the addition of antibacterial peptide V-Os could enhance the antibacterial performance of hydrogel to the greatest extent. Os is an antimicrobial peptide that has no adverse effect on eukaryotic cells, and its good antibacterial activity has been verified by many studies.^{25,26} Besides killing bacteria directly, antimicrobial peptides can inhibit the spread of bacteria and control infection by enhancing the function of immune cells such as phagocytes, neutrophils and lymphocytes in vivo. In addition, the introduction of collagen sequence into the antimicrobial polypeptide Os not only effectively improves its binding stability with the GelMA hydrogel but also does not destroy its activity, so that it can exert its biological function in the local long term and efficient. In order to further verify the antibacterial properties of different hydrogels in vivo, different hydrogels were embedded in the infected wound of rats, and the antibacterial properties of hydrogels were evaluated by tissue section method. Figure 4D shows the Gram bacteria staining results of wound skin in each group 4 days after implantation of hydrogel material, and *E. coli* can be colored blue by Gram staining. Large blue areas were found under the skin of the blank control group and the GelMA group, demonstrating that bacterial proliferation in the skin tissue. With the addition of Ti_3C_2 in the hydrogel, the blue staining area in the skin tissue was significantly reduced, but large blue areas could still be found. In the GelMA@V-Os and GelMA@ Ti_3C_2 /V-Os group, the blue areas were the smallest, and the skin tissue was basically normal.

In the process of chronic wound healing, the wound is easily infected by exogenous bacteria, and the infected wound will lead to an inflammatory response, which inhibited the formation of collagen and the regeneration of epithelial tissue. The good antibacterial ability of wound dressing can resist wound infection, so it is also an important indicator to evaluate the quality of a skin wound dressing. The above results showed that Ti_3C_2 had a certain antibacterial effect in vivo, but the antibacterial effect was significantly less than that of V-Os, which was basically consistent with the results of colony counting.

Cell Proliferation, Adhesion and Migration Assay

The existence of endogenous electric field in skin tissue makes external ES play an important role in the regeneration process of skin tissue. ES has been reported to effectively control cell function and promote tissue regeneration as a guiding signal, which can be enhanced on conductive materials, helping to achieve localized ES, so as to better regulate cell activity.^{36,37} Therefore, we studied the synergistic effect of GelMA@ Ti_3C_2 /V-Os hydrogel combined with ES on the adhesion and proliferation of NIH3T3 cells. NIH3T3 cells were inoculated on different hydrogel for 3 days with or without ES, and the cell proliferation and adhesion of the materials were observed by CCK-8 assay and Calcein AM staining. As shown in Figure 5A-D, there was no significant difference in cell proliferation between the GelMA group and the GelMA@V-Os group in the absence of ES. After adding Ti_3C_2 into the hydrogel, the cell proliferation rate was slightly improved, but there was no significant statistical difference ($P > 0.05$). These results indicated that Ti_3C_2 has good cytocompatibility and does not affect cell growth. Under the condition of ES, the cell proliferation ability of each group was increased to different degrees. When the ES voltage reached 400 mV, the cell proliferation ability began to be inhibited. Furthermore, it is found that the hydrogel group containing Ti_3C_2 had a higher cell proliferation rate under the same ES conditions. The above results demonstrated that the electroactive GelMA@ Ti_3C_2 /V-Os hydrogel could enhance the proliferation activity of NIH3T3 cells under ES, and the applied voltage of ES had strong effects on the cell behaviour. ES mainly acts on the cell membrane and increases the intracellular Ca^{2+} concentration and prostaglandin E2 levels by activating the electrovoltage-gated calcium channels on the cell membrane. ES generates electrical potentials and currents in the cytoplasm, releasing intracellular Ca^{2+} from reservoirs such as the endoplasmic reticulum. Elevated calcium ion levels activate cytoskeletal calmodulin, which in turn promotes cell proliferation and increases the expression of VEGF and transforming growth factor (TGF).³⁸ The conductive biomaterials make the ES directly act on the cells

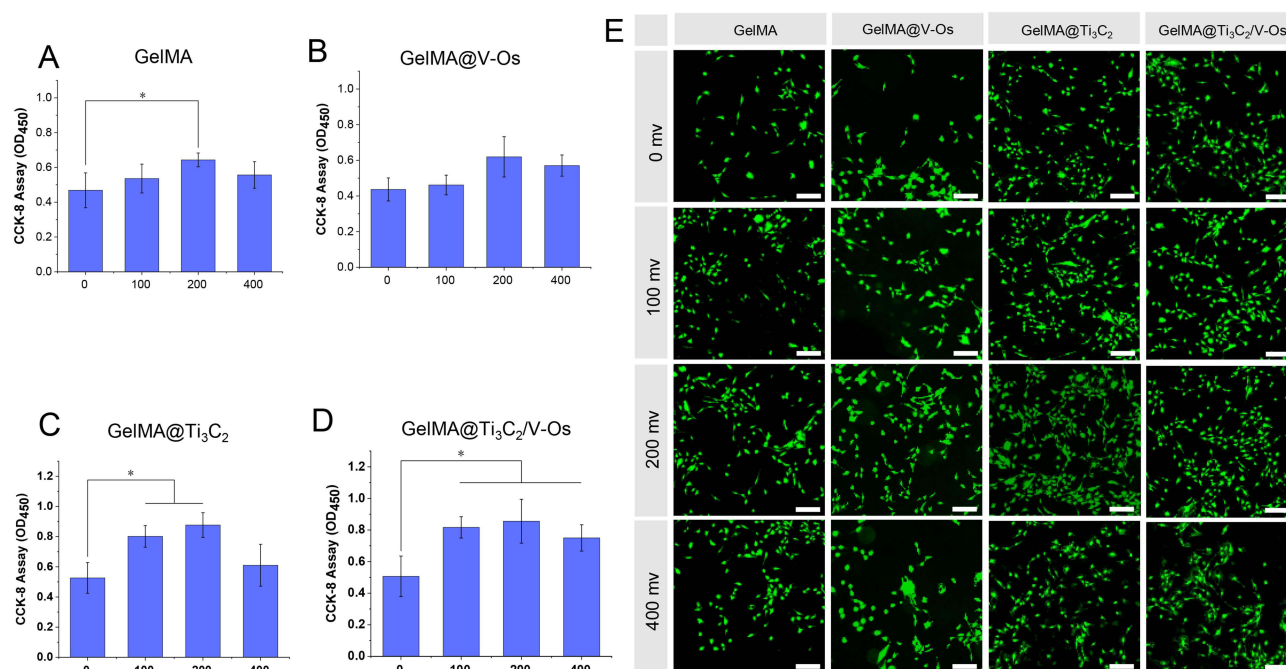


Figure 5 (A-D) cell proliferation after 4 days of culture and **(E)** cell Calcein AM staining. * $P < 0.05$, $n=3$, the scale length is 200 μ m.

and improve the efficiency of ES and electrical signal transmission between cells. In addition, ES can also modulate the adhesion behaviour of cells cultured on the GelMA@Ti₃C₂/V-Os hydrogel. As shown in Figure 5E, more adherent cells were found in all groups under ES. However, higher voltage (400 mV) was harmful to cell activity, and the number and adhesion of cells on hydrogel began to decrease. For the cells on the GelMA@Ti₃C₂ and GelMA@Ti₃C₂/V-Os group, there were significant differences under ES. Under the condition of ES, the intercellular interaction on the GelMA@Ti₃C₂ and GelMA@Ti₃C₂/V-Os hydrogel was more obvious, and the cells were stacked on each other, showing stronger adhesion behaviour. This phenomenon can be attributed to two aspects: first of all, with the addition of Ti₃C₂, the surface roughness of the hydrogel increases, providing a better anchor for cell adhesion, growth, diffusion and proliferation. Furthermore, ES can up-regulate the expression of α -smooth muscle actin in fibroblasts, thereby affecting actin, integrin and other cytoskeletal molecules that promote cell migration, thereby promoting cell migration.³⁹ Meanwhile, Ti₃C₂ is able to improve electrical conductivity of the hydrogel materials so as to better transmit physiological electrical signals to the cells, thereby helping to improve cell activity.

Cell Tissue Repair Related Genes Expression

The cell behaviours such as cell adhesion, proliferation, angiogenesis and collagen deposition are regulated by different genes, such as type I collagen (COL-I) and vascular endothelial growth factor (VEGF).²⁴ COL-I is the main structural component of the dermis, which is high in the dermis of normal skin, while VEGF is the main growth factor that promotes neovascularity. The expression of COL-I and VEGF in NIH3T3 cells grown on different hydrogels was detected by RT-PCR. As shown in Figure 6, compared with the GelMA group, the COL-I expression in GelMA@V-Os, GelMA@Ti₃C₂ and GelMA@Ti₃C₂/V-Os group increased to a certain extent, but there was no statistical difference ($P > 0.05$). The expression level of COL-I in GelMA@Ti₃C₂/V-Os+ES group was significantly higher than that in GelMA group ($P < 0.05$). Compared with GelMA group, VEGF expression in GelMA@V-Os group did not change significantly, indicating that V-Os had no significant effect on cell VEGF gene expression. In GelMA@Ti₃C₂ and GelMA@Ti₃C₂/V-Os group, cell VEGF expression was significantly increased ($P < 0.05$), indicated that Ti₃C₂ could promote cell VEGF expression to a certain extent. Under the condition of ES, cell VEGF expression of GelMA@Ti₃C₂/V-Os group was further increased, which was significantly higher than that of other groups ($P < 0.05$). When the ES is applied to the wound end of the tissue, an electrochemical reaction occurs at the electrode-tissue interface at the wound end, resulting in

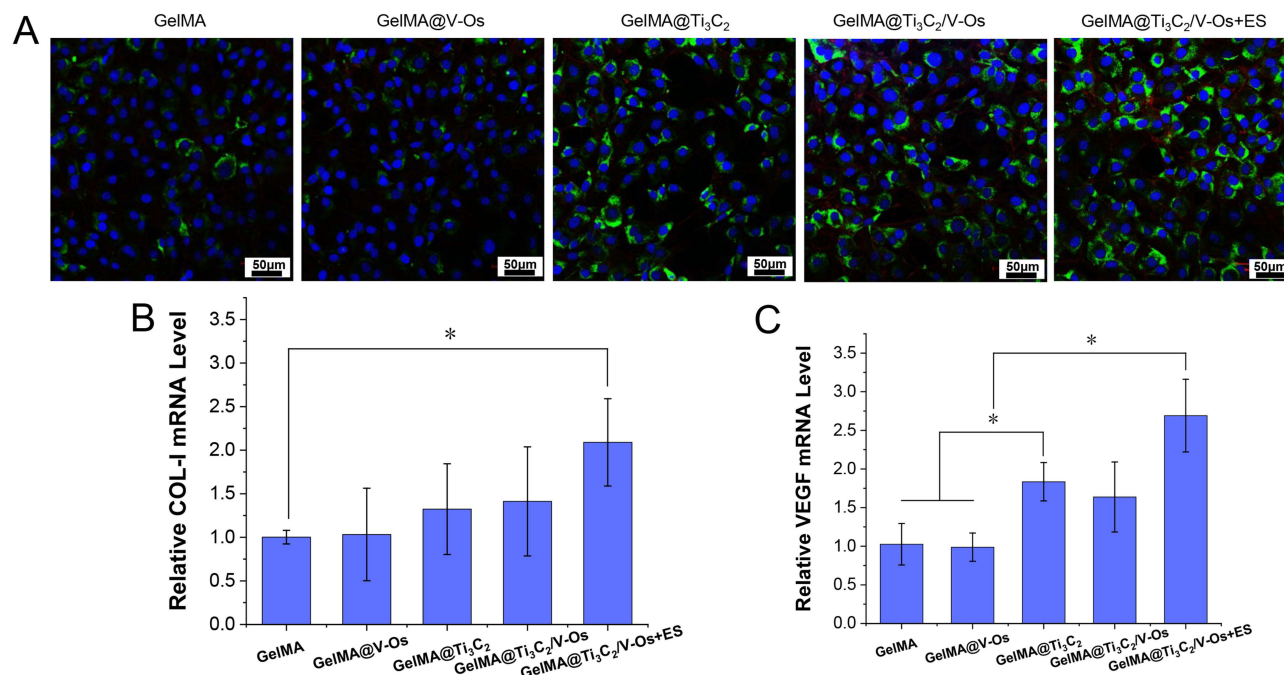


Figure 6 (A) Immunofluorescent images for COL-I expression by NIH3T3 cell seeded on different groups. Quantitative real-time PCR analysis of (B) COL-I and (C) VEGF mRNA expression levels in NIH3T3 cells seeded in different groups. * $P < 0.05$, $n=3$, the scale length is 50 μm.

an increase in oxygen consumption, and low oxygen environment can induce VEGF secretion.⁴⁰ At the same time, ES can activate mitogen-activated protein kinase and calcium channel to induce cell differentiation through VEGF.⁴¹ Ti₃C₂ in the hydrogel improves electrical conduction at the injured site, further enhancing the effect of ES. According to the results of RT-PCR, GelMA@Ti₃C₂/V-Os hydrogel and ES can synergistically up-regulate the expression of COL-I and VEGF. The effect of GelMA@Ti₃C₂/V-Os hydrogel combined with ES on the expression of cell tissue repair related genes can be explained as follows: on the one hand, GelMA@Ti₃C₂/V-Os hydrogels have good biocompatibility and physical-chemical properties, which can enhance the adsorption of proteins, and promote cell adhesion, proliferation and differentiation. On the other hand, the conductive microregions formed by Ti₃C₂ can enhance signal transduction between cells, thus significantly enhancing cell differentiation. ES can activate the opening of voltage-gated potassium channels and regulate cell membrane potential to promote ion transport, thereby promoting collagen deposition and angiogenesis.⁴²

In vivo wound Healing Assessment

In order to verify the effect of GelMA@Ti₃C₂/V-Os hydrogel and ES on tissue repair in vivo, a rat skin defect model was used to evaluate the effect of GelMA@Ti₃C₂/V-Os hydrogel and ES on skin wound healing. Figure 7A shows the external phase of rat skin wound at different time points (Day 0, 3, 6, 9, 11). On the third day, the skin wound healing of GelMA@V-Os, GelMA@Ti₃C₂ and GelMA@Ti₃C₂/V-Os groups was better than that of GelMA group, which indicated that the addition of V-Os and Ti₃C₂ could enhance the tissue repair ability of the hydrogel materials. At the 6-day point, the wound closure of GelMA@V-Os and GelMA@Ti₃C₂/V-Os groups were slightly better than GelMA@Ti₃C₂, indicated that V-Os were slightly better than Ti₃C₂ in promoting wound healing, which may be due to the fact that the addition of V-Os can inhibit bacterial growth and create a better environment for tissue regeneration. At the 11-day point, the order of wound closure effect in each group was as follows: GelMA@Ti₃C₂/V-Os+ES > GelMA@Ti₃C₂/V-Os > GelMA@V-Os > GelMA@Ti₃C₂ > GelMA group. Among all groups, GelMA@Ti₃C₂/V-Os+ES group had the best wound closure effect, which was superior to other groups. As shown in Figure 7B, quantitative analysis of wound closure rate showed that after 6 days of treatment, the wound closure rate of GelMA@Ti₃C₂/V-Os+ES, GelMA@Ti₃C₂/V-Os, GelMA@V-Os, GelMA@Ti₃C₂ and GelMA group were $72.70 \pm 6.90\%$, $67.58 \pm 11.90\%$, $72.91 \pm 6.73\%$, $60.76 \pm 5.05\%$

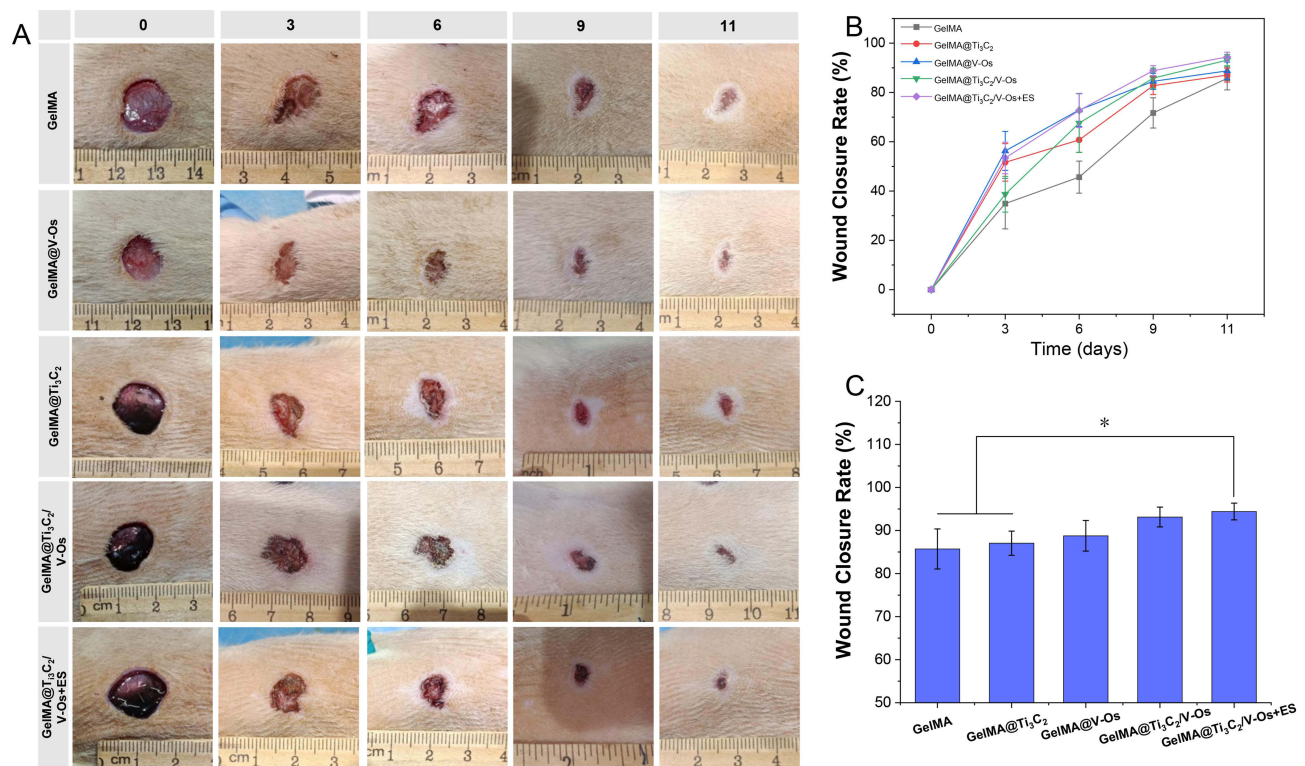


Figure 7 (A) The closure rate of the wound defects with different treatments at days 0, 3, 6, 9, and 11. (B and C) Quantitative analysis of wound closure rate % (* $P < 0.05$, $n=3$).

and $45.66 \pm 6.51\%$ respectively, and the wound closure rate in GelMA group was the lowest. After 11 days of treatment, the wound closure rate of GelMA@Ti₃C₂/V-Os+ES group was higher than that of other groups, reaching $94.41 \pm 1.95\%$ (Figure 7C). The above results showed that the tissue repair effect of ES combined with GelMA@Ti₃C₂/V-Os hydrogel was better than that of GelMA@Ti₃C₂/V-Os hydrogel on full-layer skin defects in rats.

Histologic Analysis

Wound healing is a dynamic and orderly biological process, which involves the fine regulation of many cytokines. Inflammation, collagen deposition and new tissue formation are important indicators to evaluate wound healing. In this study, we used H&E, Masson and Sirius red staining to histologically compare the healing of skin wound in each group. As shown in Figure 8A, it can be seen from the results of H&E and Masson that there are still a lot of scabs at the wound site in the GelMA group, and the epidermal reconstruction is incomplete. Furthermore, the epithelial thickness of the samples was different among the groups. The epidermis of GelMA group was thicker than that of other groups. Among all groups, the epidermis of GelMA@Ti₃C₂/V-Os+ES group was the thinnest, which was close to normal skin tissue. At the initial stage of epidermal healing, the epidermal healing gradually leads to cell proliferation and epithelial thickening. As healing continues, the epidermal thickness gradually returns to normal.⁴³ Compared with the GelMA group, the GelMA@V-Os and GelMA@Ti₃C₂/V-Os group showed more collagen deposition and less scab. The newly formed granulation tissue and keratinized layer can be clearly observed in GelMA@Ti₃C₂/V-Os+ES group, and a complete and uniform epidermal structure has been reconstructed on the surface of the wound. All these results indicated that GelMA@Ti₃C₂/V-Os+ES has a good effect on wound repair and skin tissue has entered the late stage of wound repair. At the initial stage of wound healing, type III collagen (COL-III) was the main component in the new skin tissue, while the expression of COL-I was weak.⁴⁴ With the tissue recovery process progressed, COL-III was gradually replaced by COL-I. Therefore, the ratio of COL-I to COL-III can be used as an indicator to evaluate the degree of wound healing. As shown in Figure 8B, the Sirius red results showed that most collagen in each group was COL-I. In the GelMA group, the proportion of COL-III was higher, indicated that the wound was still healing. As shown in Figure 8C and D, the proportion and content of COL-I in other groups were increased to varying

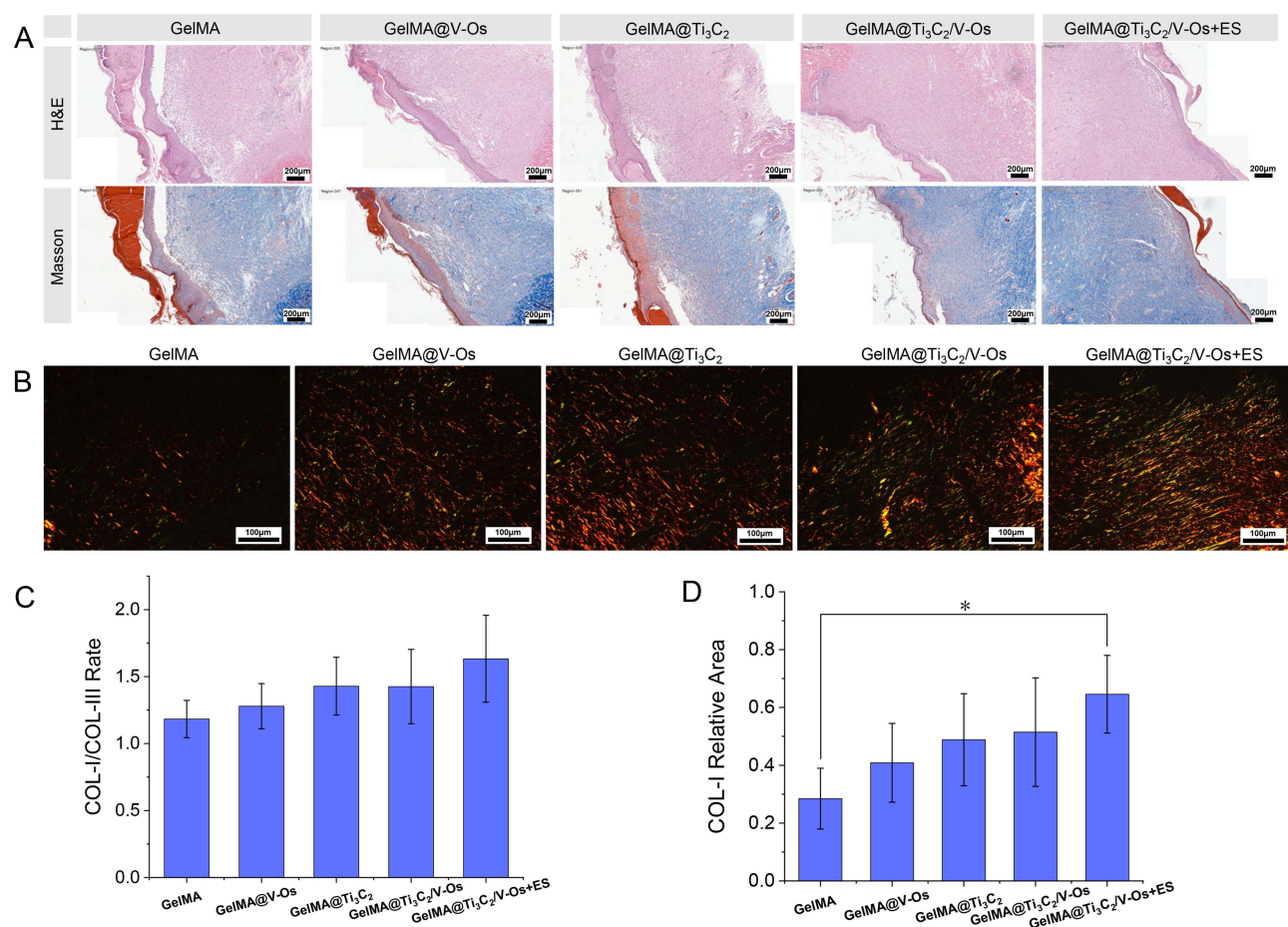


Figure 8 (A) Histomorphological evaluation of wound regeneration. (B) Image of Sirius red -stained tissue in wound healing area. (C) COL-I/COL-III area ratio in the wound-healing region. (D) COL-I contents in the wound-healing region, the scale length is 200 μm (H&E and Masson) and 100 μm (Sirius red). * $P < 0.05$, $n=3$.

degrees. The proportion and content of COL-I in GelMA@Ti₃C₂/V-Os+ES group were the highest in all groups, which was significantly higher than that in GelMA group ($P < 0.05$), which indicated that the tissue repair effect was the best, and the collagen composition in the new tissue was close to that of normal skin tissue. Some studies have found that the Ti-based molecules released from Ti₃C₂ can promote tissue growth in the presence of oxygen.⁴⁵ At the same time, Ti₃C₂ can reduce cytokine production, significantly remove reactive oxygen species (ROS), and reduce inflammation by down-regulating nuclear factor kappa B (NF-κB) and mitogen activated protein kinase (MAPK) signaling pathways. Ti₃C₂ also improved the surface roughness of the hydrogel, thus enhancing the cell adhesion of the hydrogel.⁴⁶ ES mimics the role of tissue endogenous electric field driving cell migration and enhances the expression of multiple cytokines. V-Os effectively inhibited the growth of bacteria and created a good growth environment for tissue regeneration. Under the combined action of these three effects, the healing rate and remodeling degree of skin tissue were greatly improved.

CD31 is expressed as a transmembrane protein in early angiogenesis and has also been used to evaluate vascular endothelial differentiation and angiogenesis during wound healing.⁴⁷ As shown in Figure 9A and B, CD31 was weakly positive in GelMA and GelMA@V-Os groups. The fluorescence intensity of CD31 in GelMA@Ti₃C₂ and GelMA@Ti₃C₂/V-Os groups were significantly enhanced, and new vessels was significantly increased. Among all the groups, the GelMA@Ti₃C₂/V-Os+ES group had the strongest CD31 fluorescence intensity. Tumor necrosis factor-α (TNF-α) is an inflammatory factor that occurs during the inflammatory period, which can activate the generation of neutrophils and lymphocytes, plays an important role in the inflammatory process, and serves as an indicator for evaluating inflammation.⁴⁸ Figure 9A and C shows the immunofluorescence image of TNF-α labeled tissue and the proportion of fluorescently labeled tissue in the wound tissue. The results showed that the area of TNF-α positive

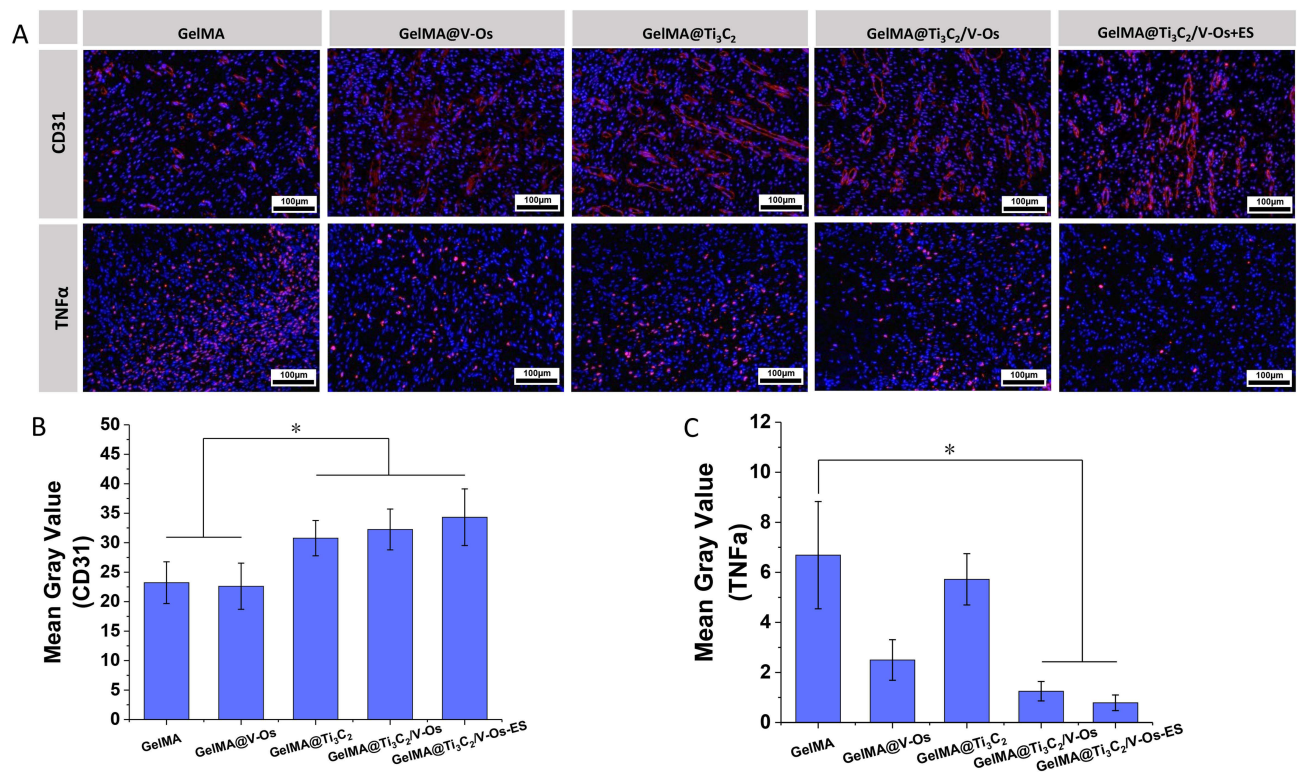


Figure 9 (A) CD31 and TNF- α staining tissue in the wound-healing region at 11 days after different treatments. The quantitative statistical analysis of (B) CD31 and (C) TNF- α relative area percentage in the wound-healing region. * $P < 0.05$, $n=3$, the scale length is 100 μ m.

tissue in the hydrogel containing V-Os treatment group was much lower than that in the GelMA and GelMA@Ti₃C₂ groups ($P < 0.05$). The slow release of V-Os reduces the expression of TNF- α , reduces the inflammation in the wound tissue, and promotes the transformation of the wound from an inflammatory phase to a proliferative phase. The above results suggest that GelMA@Ti₃C₂/V-Os hydrogel combined with ES therapy can effectively resist bacterial infection, promote granulation formation, collagen deposition, cell proliferation, vascular endothelial differentiation and angiogenesis, and ultimately significantly accelerate wound healing process.

According to wound closure rate and histological analysis, we found that GelMA@Ti₃C₂/V-Os has good tissue repair ability, but Ti₃C₂ nanomaterials can circulate into internal organs through body fluids after entering the body, and the long-term cytotoxicity of modified antibacterial peptide V-Os has not been systematically studied. Therefore, each group of hydrogel materials was implanted into the muscle of the rats, and the in vivo toxicity of the hydrogel materials was analyzed by the morphological changes of the rat internal organs. As shown in Figure 10, hearts, livers, spleens, lungs, and kidneys of rats in different groups were taken for HE staining to evaluate the toxicity of hydrogel materials. Compared with normal rats, no significant pathological changes were observed in the important organs of all experimental animals, and the organ morphology was normal. The above HE staining results showed that the prepared GelMA@Ti₃C₂/V-Os hydrogel did not cause obvious chronic toxicity in vivo.

Traditional hydrogel dressings can only play a role in physical isolation and creating a humid environment, which cannot meet the increasing requirements of clinical wound dressings. With the development of basic research, the development of multifunctional wound dressings to meet the various needs of wound repair has become the mainstream trend of wound dressing design. In this study, a multifunctional electroactive hydrogel wound dressing GelMA@Ti₃C₂/V-Os was designed to promote wound healing. GelMA@Ti₃C₂/V-Os hydrogel has shown excellent ability to accelerate skin wound healing, and the main reasons are as follows: first of all, GelMA hydrogel itself has good biocompatibility, and its photo crosslinking properties and similar extracellular matrix structure make it suitable for the treatment of irregular skin wound, providing an extracellular microenvironment for cell growth and migration. At the same time,

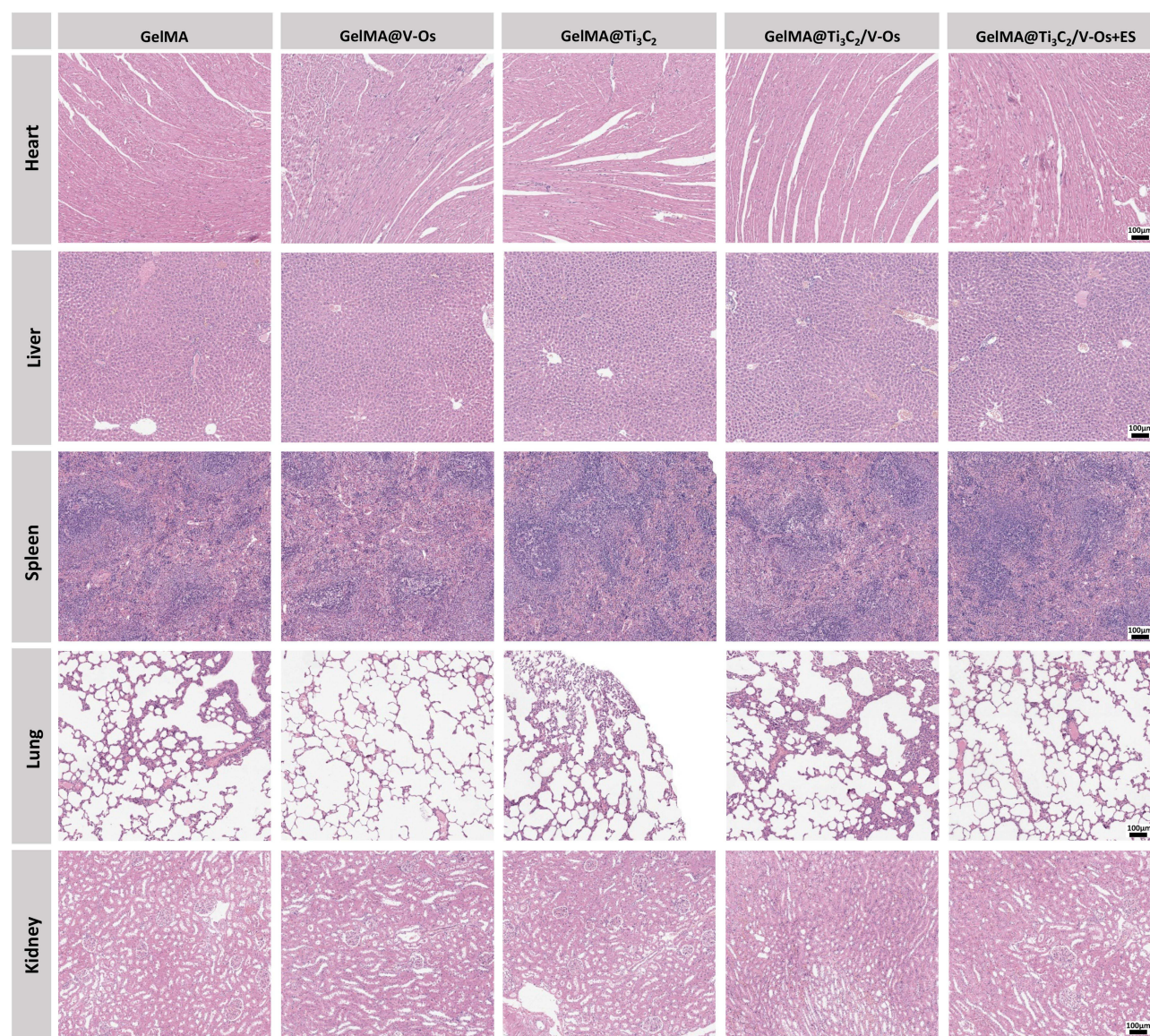


Figure 10 H&E staining sections of important organs (lung, heart, liver, spleen and kidney) in experimental animals, the scale length is 100µm.

GelMA also has good permeability and water retention. Furthermore, when Ti_3C_2 was incorporated into GelMA hydrogel, the hydrogel materials showed better biocompatibility because Ti_3C_2 could enhance the number of cell anchoring sites and reduce the inflammatory response of wound site.^{34,49} Secondly, GelMA@ Ti_3C_2 /V-Os hydrogels have good electrical conductivity, which in turn leads to the hydrogels acting as a bridge for the transmission of physiological electrical signals. At the cellular level, cell adhesion and migration are regulated by functional proteins, and the appropriate electrical signals can specifically regulate the behavior of proteins and ions.⁵⁰ At the tissue level, skin tissue has an endogenous electric field environment, and the implantation of electroactive hydrogels can provide a pathway for electrical signals between wounds and cells. In addition, due to the addition of modified antibacterial polypeptide V-Os, the hydrogel has the ability to inhibit bacterial growth during skin tissue regeneration. The improvement of the hydrogel antibacterial ability can create a more ideal cell growth environment for tissue regeneration, thus improving the rate of tissue regeneration.

In order to maximize the speed of wound healing and improve the therapeutic effect, in addition to the use of wound dressings, combined treatment with ES is another important research direction of skin wound treatment. Some studies found that ES may activate ion flow through voltage-gated ion channels (Ca^{2+} , Na^+ , K^+ , or Cl^-) and then induce different

intracellular cascades that regulate cell function and promote tissue regeneration.⁵¹ It is worth mentioning that the efficacy of ES therapy can be enhanced after the combination of electroactive materials, and the electroactive materials can help ES achieve local positioning and precise action on the damaged tissue.⁵² Our experimental results showed that conductive GelMA@Ti₃C₂/V-Os hydrogel combined with ES could synergistically promote NIH3T3 cell proliferation and tissue repair related gene expression. Using the model of full-layer skin injury in rats, we implanted GelMA@Ti₃C₂/V-Os hydrogel and applied ES to observe the tissue repair in vivo. After the electroactive hydrogel implantation in the defect area, the repair effect was obvious, and the tissue regeneration rate, collagen deposition amount and angiogenesis were improved to varying degrees, indicated that ES and electroactive GelMA@Ti₃C₂/V-Os hydrogel can synergistically promote skin tissue regeneration. These results demonstrated that the combination of exogenous ES and electroactive GelMA@Ti₃C₂/V-Os hydrogel dressings can synergistically enhance the therapeutic effect of each other. The combined application of electroactive hydrogel dressing and ES therapy provides a new idea for the treatment of skin wound and has a broad application prospect in the field of skin wound repair.

Conclusion

In this study, we have demonstrated that a new hydrogel based on GelMA, Ti₃C₂ and V-Os as a wound dressing can accelerate the healing process of skin wounds under external ES. The internal composition of hydrogel was confirmed by FTIR, XPS and polypeptide binding experiments. SEM and micro-CT detection showed that GelMA@Ti₃C₂/V-Os hydrogel showed obvious loose porous structure. Ti₃C₂ and V-Os endow hydrogel materials a variety of functions, such as good biocompatibility, hydrophilicity and conductivity. GelMA@Ti₃C₂/V-Os hydrogel can be used as an electroactive matrix to transmit electrical signals and regulate cell activities. Furthermore, the results of polypeptide binding experiment and antibacterial activity analysis showed that V-Os can bind more closely to GelMA hydrogel materials, thereby exerting long-lasting antibacterial effect, inhibiting bacterial growth and creating favorable conditions for tissue regeneration. In the presence of exogenous ES, the synergistic effect of GelMA@Ti₃C₂/V-Os hydrogel and ES can significantly improve the cell activity of NIH3T3 cells in vitro, promote cell proliferation and the expression of tissue repair related genes and proteins, and actively promote the wound healing process in vivo, which is reflected in the decrease of wound area and inflammatory cells, and the increase of collagen deposition and vascularization. In conclusion, the electroactive GelMA@Ti₃C₂/V-Os hydrogel is a promising wound dressing for skin wound healing. At the same time, this study provides the skin wound treatment strategy of electroactive hydrogel combined with ES, which is of great significance for clinical skin wound treatment.

Disclosure

The authors report no conflicts of interest in this work.

References

1. Das S, Baker AB. Biomaterials and Nanotherapeutics for Enhancing Skin Wound Healing. *Front Bioeng Biotechnol*. 2016;4:20. doi:10.3389/fbioe.2016.00082
2. Liang CZ, He J, Cao Y, et al. Advances in the application of Mxene nanoparticles in wound healing. *J Biol Eng*. 2023;17(1). doi:10.1186/s13036-023-00355-7
3. Mohammadnejad H, Abbaszadeh S, Sefat F, et al., Dermal Wound Healing. In: *Electrically Conducting Polymers and Their Composites for Tissue Engineering*. Vol. 1438. American Chemical Society; 2023:137–158.
4. Zhao NY, Yuan WZ. Antibacterial, conductive nanocomposite hydrogel based on dextran, carboxymethyl chitosan and chitosan oligosaccharide for diabetic wound therapy and health monitoring. *Int J Biol Macromol*. 2023;253. doi:10.1016/j.ijbiomac.2023.126625
5. Gao C, Zhang L, Wang J, et al. Electrospun nanofibers promote wound healing: theories, techniques, and perspectives†. *J Mat Chem B*. 2021;9(14):3106–3130. doi:10.1039/d1tb00067e
6. Zhou YP, Li HY, Liu JW, et al. Acetate chitosan with CaCO₃ doping form tough hydrogel for hemostasis and wound healing. *Polym Adv Technol*. 2019;30(1):143–152. doi:10.1002/pat.4452
7. Zhang YW, Jiang MM, Zhang YQ, et al. Novel lignin-chitosan-PVA composite hydrogel for wound dressing. *Mater Sci Eng C-Mater Biol Appl*. 2019;104:8. doi:10.1016/j.msec.2019.110002
8. Noori Tahneh A, Dashtipour B, Ghofrani A, et al. Crosslinked natural hydrogels for drug delivery systems. *J Composites Compounds*. 2022;4(11):109–123. doi:10.52547/jcc.4.2.6
9. Thakral G, Lafontaine J, Najafi B, et al. Electrical stimulation to accelerate wound healing. *Diabetic Foot & Ankle*. 2013;4. doi:10.3402/dfa.v4i0.22081
10. Gardner SE, Frantz RA, Schmidt FL. Effect of electrical stimulation on chronic wound healing: a meta-analysis. *Wound Repair Regener*. 1999;7(6):495–503. doi:10.1046/j.1524-475X.1999.00495.x

11. Sun GX, Wang LJ, Xiang C, et al. A dynamic model for intracellular calcium response in fibroblasts induced by electrical stimulation. *Math Biosci.* 2013;244(1):47–57. doi:10.1016/j.mbs.2013.04.005
12. Min JH, Patel M, Koh WG. Incorporation of Conductive Materials into Hydrogels for Tissue Engineering Applications. *Polymers.* 2018;10(10). doi:10.3390/polym10101078
13. Ruan J, Wang XS, Yu Z, et al. Enhanced Physiochemical and Mechanical Performance of Chitosan-Grafted Graphene Oxide for Superior Osteoinductivity. *Adv. Funct. Mater.* 2016;26(7):1085–1097. doi:10.1002/adfm.201504141
14. Gupta A, Amerei Bozcheloei Z, Ghofrani A, et al. Electroactive composite for wound dressing. *J Composites Compounds.* 2022;4(10):13–23. doi:10.52547/jcc.4.1.3
15. Rafieerad A, Yan WA, Sequiera GL, et al. Application of Ti_3C_2 MXene Quantum Dots for Immunomodulation and Regenerative Medicine. *Adv. Healthcare Mater.* 2019;569. doi:10.1002/adhm.201900569
16. Yin JH, Pan SS, Guo X, et al. Nb 2C MXene-Functionalized Scaffolds Enables Osteosarcoma Phototherapy and Angiogenesis/Osteogenesis of Bone Defects. *Nano-Micro Lett.* 2021;13(1). doi:10.1007/s40820-020-00547-6
17. Zhou L, Zheng H, Liu ZX, et al. Conductive Antibacterial Hemostatic Multifunctional Scaffolds Based on $\text{Ti}_3\text{C}_2\text{Tx}$ MXene Nanosheets for Promoting Multidrug-Resistant Bacteria-Infected Wound Healing. *ACS Nano.* 2021;15(2):2468–2480. doi:10.1021/acsnano.0c06287
18. Lu SY, Meng G, Wang C, et al. Photocatalytic inactivation of airborne bacteria in a polyurethane foam reactor loaded with a hybrid of MXene and anatase TiO_2 exposing {001} facets. *Chem Eng J.* 2021;404. doi:10.1016/j.cej.2020.126526
19. Li Y, Fu RZ, Duan ZG, et al. Artificial Nonenzymatic Antioxidant MXene Nanosheet-Anchored Injectable Hydrogel as a Mild Photothermal-Controlled Oxygen Release Platform for Diabetic Wound Healing. *ACS Nano.* 2022;16(5):7486–7502. doi:10.1021/acsnano.1c10575
20. Zhang T, Liu F, Tian W. Advance of new dressings for promoting skin wound healing. *J Biomed Eng.* 2019;36(6):1055–1059. doi:10.7507/1001-5515.201811023
21. Bessa LJ, Fazii P, Di Giulio M, et al. Bacterial isolates from infected wounds and their antibiotic susceptibility pattern: some remarks about wound infection. *Int Wound J.* 2015;12(1):47–52. doi:10.1111/iwj.12049
22. Reddy KVR, Yedery RD, Aranha C. Antimicrobial peptides: premises and promises. *Int J Antimicrob Agents.* 2004;24(6):536–547. doi:10.1016/j.ijantimicag.2004.09.005
23. Wang Y, Fu C, Wu ZX, et al. A chitin film containing basic fibroblast growth factor with a chitin-binding domain as wound dressings. *Carbohydr. Polym.* 2017;174:723–730. doi:10.1016/j.carbpol.2017.05.087
24. Zhan J, Xu H, Zhong Y, et al. Surface modification of patterned electrospun nanofibrous films via the adhesion of DOPA-bFGF and DOPA-ponericin G1 for skin wound healing. *Mater Des.* 2020;188. doi:10.1016/j.matdes.2019.108432
25. Taute H, Bester MJ, Gaspar ARM. The dual functionality of antimicrobial peptides Os and Os-C in human leukocytes. *J Pept Sci.* 2019;25(4):10. doi:10.1002/psc.3156
26. Taute H, Bester MJ, Neitz AWH, et al. Investigation into the mechanism of action of the antimicrobial peptides Os and Os-C derived from a tick defensin. *Peptides.* 2015;71:179–187. doi:10.1016/j.peptides.2015.07.017
27. Zhang J, Li J, Jia G, et al. Improving osteogenesis of PLGA/HA porous scaffolds based on dual delivery of BMP-2 and IGF-1 via a polydopamine coating. *RSC Adv.* 2017;7(89):56732–56742. doi:10.1039/c7ra12062a
28. Yang CS, Zhou L, Geng XD, et al. New dual-function *in situ* bone repair scaffolds promote osteogenesis and reduce infection. *J Biol Eng.* 2022;16(1). doi:10.1186/s13036-022-00302-y
29. Fu C, Qi Z, Zhao C, et al. Enhanced wound repair ability of arginine-chitosan nanocomposite membrane through the antimicrobial peptides-loaded polydopamine-modified graphene oxide. *J Biol Eng.* 2021;15(1). doi:10.1186/s13036-021-00268-3
30. Mao L, Hu S, Gao Y, et al. Biodegradable and Electroactive Regenerated Bacterial Cellulose/MXene ($\text{Ti}_3\text{C}_2\text{Tx}$) Composite Hydrogel as Wound Dressing for Accelerating Skin Wound Healing under Electrical Stimulation. *Adv. Healthcare Mater.* 2020;9(19). doi:10.1002/adhm.202000872
31. Serafin A, Culebras M, Oliveira JM, et al. 3D printable electroconductive gelatin-hyaluronic acid materials containing polypyrrole nanoparticles for electroactive tissue engineering. *Adv. Compos. Hybrid Mater.* 2023;6(3). doi:10.1007/s42114-023-00665-w
32. Ning CY, Zhou ZN, Tan GX, et al. Electroactive polymers for tissue regeneration: developments and perspectives. *Prog Polym Sci.* 2018;81:144–162. doi:10.1016/j.progpolymsci.2018.01.001
33. Shamsabadi AA, Gh MS, Anasori B, et al. Antimicrobial Mode-of-Action of Colloidal $\text{Ti}_3\text{C}_2\text{Tx}$ MXene Nanosheets. *ACS Sustainable Chem. Eng.* 2018;6(12):16586–16596. doi:10.1021/acssuschemeng.8b03823
34. Abbasi F, Hajilary N, Rezakazemi M. Antibacterial properties of MXene-based nanomaterials: a review. *Materials Express.* 2022;12(1):34–48. doi:10.1166/mex.2022.2138
35. Pandey RP, Rasheed PA, Gomez T, et al. Effect of Sheet Size and Atomic Structure on the Antibacterial Activity of Nb-MXene Nanosheets. *ACS Appl. Nano Mater.* 2020;3(11):11372–11382. doi:10.1021/acsanm.0c02463
36. Qi ZP, Xia P, Pan S, et al. Combined treatment with electrical stimulation and insulin-like growth factor-1 promotes bone regeneration *In vitro*. *PLoS One.* 2018;13(5):17. doi:10.1371/journal.pone.0197006
37. Wang Y, Cui HT, Wu ZX, et al. Modulation of Osteogenesis in MC3T3-E1 Cells by Different Frequency Electrical Stimulation. *PLoS One.* 2016;11(5):4924. doi:10.1371/journal.pone.0154924
38. Chen C, Bai X, Ding Y, et al. Electrical stimulation as a novel tool for regulating cell behavior in tissue engineering. *Biomater Res.* 2019;23(1):176. doi:10.1186/s40824-019-0176-8
39. Abedin-Do A, Zhang Z, Douville Y, et al. Electrical stimulation promotes the wound-healing properties of diabetic human skin fibroblasts. *J Tissue Eng Regen Med.* 2022;16(7):643–652. doi:10.1002/term.3305
40. Hoppeler H. Vascular growth in hypoxic skeletal muscle. In: Roach RC, Wagner PD, Hackett PH, editors. *Hypoxi: Into the Next Millennium*. Vol. 474. 1999:277–286.
41. Kim IS, Song JK, Song YM, et al. Novel Effect of Biphasic Electric Current on *In vitro* Osteogenesis and Cytokine Production in Human Mesenchymal Stromal Cells. *Tissue Eng Part A.* 2009;15(9):2411–2422. doi:10.1089/ten.tea.2008.0554
42. Franklin BM, Maroudas E, Osborn JL. Sine-wave electrical stimulation initiates a voltage-gated potassium channel-dependent soft tissue response characterized by induction of hemocyte recruitment and collagen deposition. *Physiological Reports.* 2016;4(12):832. doi:10.14814/phy2.12832
43. You D, Li K, Guo WL, et al. Poly (lactic-co-glycolic acid)/graphene oxide composites combined with electrical stimulation in wound healing: preparation and characterization. *Int j Nanomed.* 2019;14:7039–7052. doi:10.2147/ijn.s216365

44. Li J, Chen J, Kirsner R. Pathophysiology of acute wound healing. *Clin Dermatol*. 2007;25(1):9–18. doi:10.1016/j.clindermatol.2006.09.007
45. Zhang J, Fu Y, Mo A. Multilayered Titanium Carbide MXene Film for Guided Bone Regeneration. *Int j Nanomed*. 2019;14:10091–10102. doi:10.2147/ijn.S227830
46. Huang Y, He S, Yu S, et al. MXene-Decorated Nanofibrous Membrane with Programmed Antibacterial and Anti-Inflammatory Effects via Steering NF- κ B Pathway for Infectious Cutaneous Regeneration. *Small*. 2024;20(4):119. doi:10.1002/sml.202304119
47. Zhao L, Feng Z, Lyu Y, et al. Electroactive injectable hydrogel based on oxidized sodium alginate and carboxymethyl chitosan for wound healing. *Int J Biol Macromol*. 2023;230. doi:10.1016/j.ijbiomac.2023.123231
48. Fu X, Tian H, Hsu S, et al. *In vivo* effects of tumor necrosis factor- α on incised wound and gunshot wound healing. *J Trauma*. 1996;40(3 Suppl):S140–3. doi:10.1097/00005373-199603001-00030
49. Nie R, Sun Y, Lv HX, et al. 3D printing of MXene composite hydrogel scaffolds for photothermal antibacterial activity and bone regeneration in infected bone defect models. *Nanoscale*. 2022;14(22):8112–8129. doi:10.1039/d2nr02176e
50. Wu CH, Liu A, Chen SP, et al. Cell-Laden Electroconductive Hydrogel Simulating Nerve Matrix To Deliver Electrical Cues and Promote Neurogenesis. *ACS Appl. Mater. Interfaces*. 2019;11(25):22152–22163. doi:10.1021/acsami.9b05520
51. Chen C, Bai X, Ding Y, et al. Electrical stimulation as a novel tool for regulating cell behavior in tissue engineering. *Biomater Res*. 2019;23:25. doi:10.1186/s40824-019-0176-8
52. Tang P, Han L, Li P, et al. Mussel-Inspired Electroactive and Antioxidative Scaffolds with Incorporation of Polydopamine-Reduced Graphene Oxide for Enhancing Skin Wound Healing. *ACS Appl. Mater. Interfaces*. 2019;11(8):7703–7714. doi:10.1021/acsami.8b18931

International Journal of Nanomedicine

Dovepress

Publish your work in this journal

The International Journal of Nanomedicine is an international, peer-reviewed journal focusing on the application of nanotechnology in diagnostics, therapeutics, and drug delivery systems throughout the biomedical field. This journal is indexed on PubMed Central, MedLine, CAS, SciSearch®, Current Contents®/Clinical Medicine, Journal Citation Reports/Science Edition, EMBase, Scopus and the Elsevier Bibliographic databases. The manuscript management system is completely online and includes a very quick and fair peer-review system, which is all easy to use. Visit <http://www.dovepress.com/testimonials.php> to read real quotes from published authors.

Submit your manuscript here: <https://www.dovepress.com/international-journal-of-nanomedicine-journal>